Alteration of Gene Expression in Pathological Keratinization of the Ocular Surface

Hokoru Yoshioka,[1] Mayumi Ueta,[1] Hideki Fukuoka,[1] Norihiko Yokoi,[1] Katsura Mizushima,[2] Yuji Naito,[2] Shigeru Kinoshita,[3] and Chie Sotozono[1]

[1]Department of Ophthalmology, Kyoto Prefectural University of Medicine, Kyoto, Japan
[2]Department of Human Immunology and Nutrition Science, Graduate School of Medical Science, Kyoto Prefectural University of Medicine, Kamigyo-ku, Kyoto, Japan
[3]Department of Frontier Medical Science and Technology for Ophthalmology, Kyoto Prefectural University of Medicine, Kyoto, Japan

Correspondence: Chie Sotozono, Department of Ophthalmology, Kyoto Prefectural University of Medicine, 465 Kajii-cho, Kamigyo-ku, Kyoto 602-8566, Japan; csotozon@koto.kpu-m.ac.jp.

Received: December 16, 2023
Accepted: June 3, 2024
Published: June 27, 2024

Citation: Yoshioka H, Ueta M, Fukuoka H, et al. Alteration of gene expression in pathological keratinization of the ocular surface. *Invest Ophthalmol Vis Sci.* 2024;65(6):37. https://doi.org/10.1167/iovs.65.6.37

Purpose. To investigate the molecular mechanism of pathological keratinization in the chronic phase of ocular surface (OS) diseases.

Methods. In this study, a comprehensive gene expression analysis was performed using oligonucleotide microarrays on OS epithelial cells obtained from three patients with pathological keratinization (Stevens-Johnson syndrome [n = 1 patient], ocular cicatricial pemphigoid [n = 1 patient], and anterior staphyloma [n = 1 patient]). The controls were three patients with conjunctivochalasis. The expression in some transcripts was confirmed using quantitative real-time PCR.

Results. Compared to the controls, 3118 genes were significantly upregulated by a factor of 2 or more than one-half in the pathological keratinized epithelial cells (analysis of variance $P < 0.05$). Genes involved in keratinization, lipid metabolism, and oxidoreductase were upregulated, while genes involved in cellular response, as well as known transcription factors (TFs), were downregulated. Those genes were further analyzed with respect to TFs and retinoic acid (RA) through gene ontology analysis and known reports. The expression of TFs MYBL2, FOXM1, and SREBF2, was upregulated, and the TF ELF3 was significantly downregulated. The expression of AKR1B15, RDH12, and CRABP2 (i.e., genes related to RA, which is known to suppress keratinization) was increased more than twentyfold, whereas the expression of genes RARB and RARRES3 was decreased by 1/50. CRABP2, RARB, and RARRES3 expression changes were also confirmed by qRT-PCR.

Conclusions. In pathological keratinized ocular surfaces, common transcript changes, including abnormalities in vitamin A metabolism, are involved in the mechanism of pathological keratinization.

Keywords: ocular surface disease, keratinization, retinoic acid receptor beta (RARB), vitamin A

Ocular surface (OS) diseases (OSDs) such as Stevens-Johnson syndrome (SJS) and ocular cicatricial pemphigoid (OCP), as well as thermal/chemical injuries, are very devastating ocular disorders, and the associated prolonged OS inflammation can cause further damage to the residual limbal stem cells, thus inducing limbal stem cell deficiency. In the most severe OSD cases, the conjunctival epithelium and goblet cells can also be compromised, thus resulting in severe dry eye disease with keratinization and symblepharon in addition to severe aqueous tear deficiency via the involvement of lacrimal gland ducts in the subconjunctival scarring.[1–4]

SJS is a systemic disease characterized by acute inflammatory vesiculobullous reaction of the skin, OS, and oral cavity, and is termed "toxic epidermal necrolysis" (i.e., the more severe variant of SJS) when the disease affects a larger surface area of the body.[2,3,5] OCP is a type of pemphigoid of the mucosa characterized by chronic, recurrent, and progressive conjunctivitis. In the chronic phase of these OSDs, OS inflammation persists, as do OS complications such as severe dry eye, eyelash disorders, and conjunctival invasion.[1,3,4,6]

In cases of severe OSD, pathological keratinization develops on the OS, resulting in severe vision loss. Despite the variety of surgical procedures currently available and the advanced methods of postoperative management that have recently been developed, OS reconstruction in cases of severe OSD, including those with keratinization, remains one of the most challenging procedures in ophthalmology.[7]

The pathologic transformation from nonkeratinizing to keratinizing epithelium is termed 'squamous metaplasia'. In the OS, squamous metaplasia leads to loss of goblet cells, stratification of the epithelium, and pathological keratinization, and it has reportedly been found in various OSDs, such as SJS, OCP, thermal/chemical injury, and dry eye disease associated with Sjögren's syndrome, as well as in vitamin A deficiency cases.[8,9]

We hypothesized that although various pathological conditions are involved in OS keratinization, a common mechanism occurs for transformation to keratinizing epithelial cells. In this study, we clinically examined OSD cases with pathological keratinization of the OS to identify the expressed proteins via immunostaining and comprehensive microarray gene expression analysis to clarify the underlying process that leads to pathological keratinization.

Material and Methods

Patient and Public Involvement

The protocols of this study were approved by the Institutional Review Board of Kyoto Prefectural University of Medicine, Kyoto, Japan, and written informed consent was obtained from all participants before their involvement in the study. All study procedures were conducted in accordance with the tenets set forth in the Declaration of Helsinki.

This study involved three severe OSD patients (a 79-year-old woman with OCP, a 23-year-old man with SJS, and a 10-month-old male infant with anterior staphyloma who presented with severe keratinization) seen at the Department of Ophthalmology of Kyoto Prefectural University of Medicine. In all three cases, conjunctival invasion and subsequent pathological keratinization had occurred, so surgical OS reconstruction was performed to restore the conjunctival fornix and improve visual acuity,[10] and a conjunctival tissue sample was obtained at the time of surgery. In addition, in the patient who had difficulty closing his eyelid because of anterior staphyloma with resultant gradual keratinization of the OS, a keratinized sample was obtained after exenterating the bulbar for the purpose of an ocular prosthesis stretched to enhance the development of the fornix and orbit (Fig. 1).[11] The control subjects in this study were three female patients (age 45, 73, and 79 years) with conjunctivochalasis. In all three patients, a conjunctival tissue sample was obtained during conjunctivochalasis surgery.

Human Conjunctival Epithelium

Conjunctival epithelial tissue was immersed in 1.0 U/mL of Dispase II (FUJIFILM Wako Pure Chemical Corporation, Osaka, Japan) overnight at 4°C to isolate epithelial cells.

Morphological Evaluation and Immunohistochemistry

For morphological evaluation and immunohistochemistry, tissue samples were obtained from the 23-year-old man with SJS and the 10-month-old male infant with anterior staphyloma. Briefly, the samples were first frozen-embedded with optimal cutting temperature compound and sectioned, and then fixed in methanol at 4°C for 10 minutes, washed with PBS, and permeabilized with 0.5% Triton X-100 (Thermo Fischer Scientific, Inc., Waltham, MA, USA)/0.01 M PBS for 15 minutes. Hematoxylin-eosin (H&E) staining was then used for morphological evaluation. All immunostaining was performed using mouse IgG antibodies as the primary antibodies, with the samples then being incubated overnight at 4°C under a moist condition. The primary antibodies used in this study were cytokeratin (CK)-1 (CK1), CK10 (both obtained from Santa Cruz Biotechnology, Santa Cruz, CA, USA), CK13 (obtained from Invitrogen Corporation, Carlsbad, CA, USA), and filaggrin (obtained from Biogenesis, Westminster, CO, USA). After the slides were washed, secondary antibodies were incubated with Alexa Fluor 488 donkey anti-mouse IgG (Life Technologies Corporation, San Diego, CA, USA) for one hour at room temper-

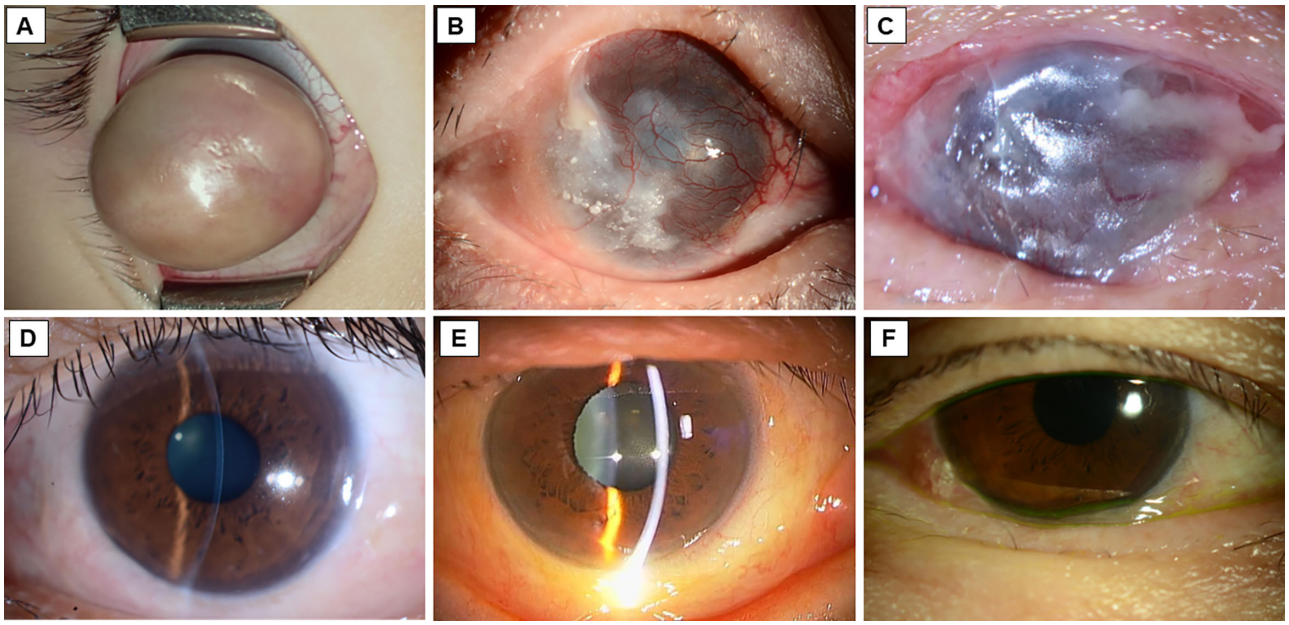

Figure 1. Photographs of the eyes of three patients with OS keratinization (**A–C**) and the three control patients with conjunctivochalasis (**D–F**). (**A**) Intraoperative photo of the eye of a patient with anterior staphyloma that resulted in an eyelid closure disorder and the progressive development of skin-like keratinization. The patient underwent exenteration of the bulbar for the purpose of an ocular prosthesis stretched to enhance the development of the fornix and orbit. (**B**) The eye of an SJS patient with symblepharon, trichiasis, conjunctival invasion, and clinical keratinization. (**C**) The eye of a patient with OCP that resulted in conjunctival invasion because of limbal stem cell deficiency, symblepharon, and clinical keratinization. (**D–F**) Images of the eyes of the three control patients with inferior conjunctivochalasis.

Investigative Ophthalmology & Visual Science

ature for staining. The slides were once again washed and then encapsulated with an anti-fading encapsulant (Nacalai Tesque, Inc., Kyoto, Japan) containing DAPI (4′,6-diamidino-2-phenylindole).

Gene Expression Analysis

Gene expression analysis was performed using high-density oligonucleotide arrays (Clariom S Array, human ; Applied Biosystems, Waltham, MA, USA) for 21,448 genes. Total RNA of isolated epithelial cells was first isolated using the RNeasy Plus Mini Kit (Qiagen, Inc., Valencia, CA, USA) or TRIzol Reagent (Thermo Fisher Scientific, Waltham, MA, USA) and then purified using the NucleoSpin RNA Clean-up XS (Macherey-Nagel GmbH & Co. KG, Dueren, Germany) kit. Microarray experiments were then performed according to the protocols provided by Thermo Fisher Scientific, and scanned microarray images were obtained using the GeneChip Scanner 3000 7G (Thermo Fisher Scientific) microarray analysis system.

Quantitative Real-Time PCR

Isolated total RNA was reverse transcribed using the QuantiTect Reverse Transcription Kit (Qiagen, Hilden, Germany). QRT-PCR was performed on a StepOnePlus (Applied Biosystems) RT-PCR system according to the manufacturer's instructions. The primers used in this study are listed in Supplementary Table S1. Quantitative comparisons were performed by normalizing for the expression of the housekeeping gene 18S.

Data Analysis

Microarray data was normalized using the Transcriptome Analysis Console v.4.0.3 (Thermo Fisher Scientific) to identify genes with statistically significant changes in gene expression (P value [analysis of variance {ANOVA}, false discovery rate {FDR}] < 0.05, $|\text{Fold Change}| > 2$). Principal component analysis plots and Volcano plots were plotted using the Transcriptome Analysis Console. Gene ontology (GO) analysis was performed using DAVID (Database for Annotation, Visualization and Integrated Discovery) (https://david.ncifcrf.gov) for genes with significant expression change (FDR < 0.05, $P < 0.05$), and charted using the QuickGO browser (https://www.ebi.ac.uk/QuickGO/) from the 10 GO terms with the lowest P values. Enrichment analysis was performed using ChIP-Atlas (https://chip-atlas.org) to analyze upstream transcription factors (TFs). QRT-PCR was analyzed using the t-test, and a P value < 0.05 was considered statistically significant. All statistical analyses were performed using EZR (Easy R) (Saitama Medical Center, Jichi Medical University, Saitama, Japan) statistics software (i.e., a graphical user interface for R ; The R Foundation for Statistical Computing, Vienna, Austria) that adds statistical functions frequently used in biostatistics.[12]

Results

Morphological Evaluation and Immunohistochemistry

In the two OSD patients with OCP, SJS, and anterior staphyloma, respectively, the conditions worsened over time, thus ultimately leading to pathological keratinization (Fig. 1). The three control patients with conjunctivochalasis who had pathologically nonkeratinized conjunctiva are included Figure 1 for comparison.

Morphological evaluation of the keratinized samples (SJS and anterior staphyloma) was performed using H&E staining, and expression of CK and filaggrin in the pathological keratinization was evaluated by immunohistochemistry (Fig. 2). The keratinized cases were highly stratified, forming a cornified envelope with some nucleus containing cells.

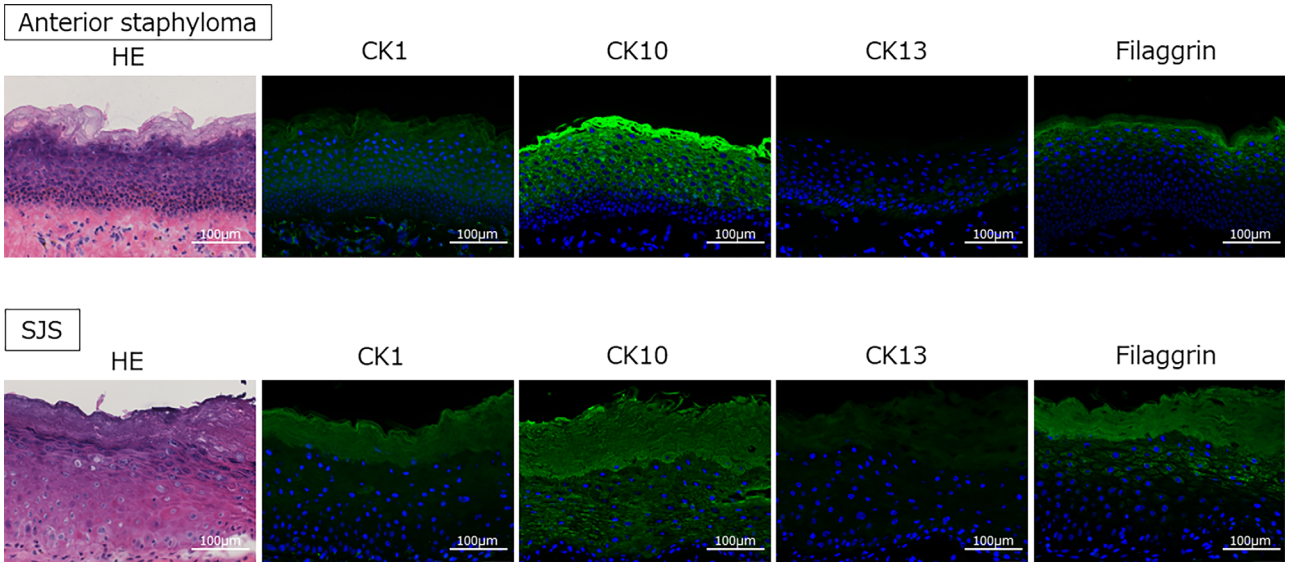

Figure 2. H&E and immunostaining images of representative cases of anterior staphyloma (*top row*) and SJS (*bottom row*) with OS keratinization. In the anterior staphyloma patient, thickened tissue over the cornea-like tissue was sectioned. In the SJS patient, sections were prepared from tissue from the peripheral cornea to the conjunctiva. In both cases, the more superficial tissues cornified, but the cornified layer also showed hyperkeratosis with some nucleus containing cells. CK-13, a marker of nonkeratinized mucosal epithelium, lost its staining, and the staining of keratinization markers CK1, CK10, and filaggrin was highly elevated. *Scale bar*: 100 μm.

Investigative Ophthalmology & Visual Science

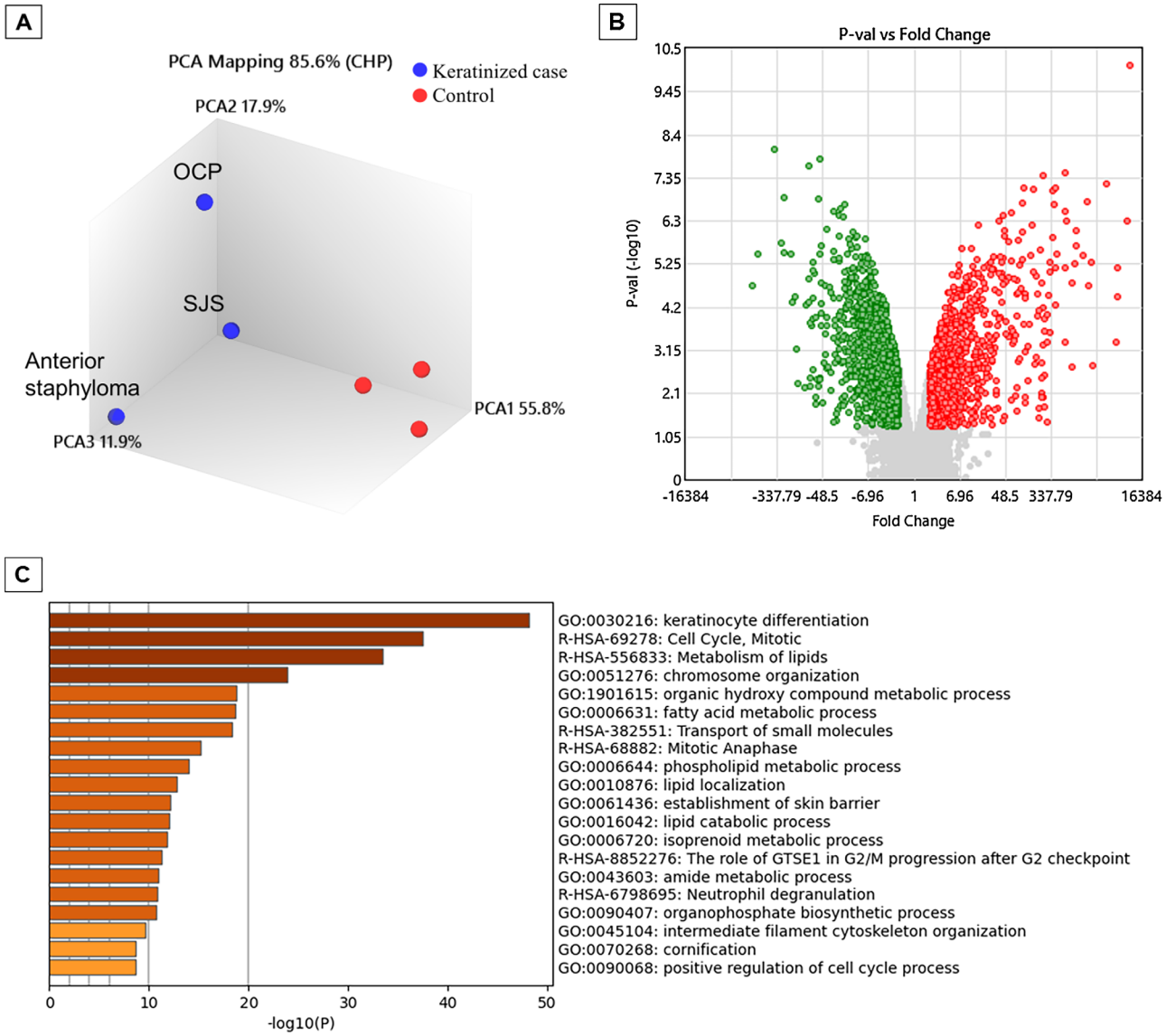

Figure 3. Image showing the results of the comprehensive gene expression analysis in the three patients with OS keratinization (i.e., anterior staphyloma, SJS, and OCP) and the three control patients. The results of the gene expression analysis using microarrays were normalized using the Transcriptome Analysis Console (QIAGEN) to identify genes with statistically significant changes in gene expression (*P* value [ANOVA], FDR < 0.05, |Fold Change| > 2). An analysis console was used for mapping the principal component analysis (PCA) plots (**A**) and Volcano plots (**B**). In the clinical keratinized cases, 1272 genes were significantly upregulated (*red dots*), and 1846 genes were significantly downregulated (*green dots*) (**B**). Using the Metascape web-based portal (https://www.metascape.org) to analyze genes significantly upregulated in clinical keratinization, we first identified all statistically enriched terms (i.e., GO/KEGG terms, canonical pathways, hallmark gene sets, etc., based on default selections in Express Analysis). Then, accumulative hypergeometric *P* values and enrichment factors were computed and used for filtering. The remaining significant terms were clustered hierarchically in a tree based on kappa statistical similarity between gene members. A kappa score of 0.3 was then applied as a threshold to classify the tree into term clusters (**C**). In the biological process and molecular function, enrichment analysis was performed using DAVID (https://david.ncifcrf.gov) on the significantly upregulated genes to obtain the top 10 *P* values of GO terms, and charts were created. The QuickGO browser (https://www.ebi.ac.uk/QuickGO/) was used for charting (**D** and **E**).

The expression of CK1, CK10, and filaggrin (all three being keratinization markers) were elevated, whereas the expression of CK13 (a marker of nonkeratinization) was decreased.

Transcriptome Analysis

For comparison of the upregulated and downregulated transcripts in the three keratinized cases and the three control cases, comprehensive gene expression analysis using microarrays was performed in all six cases. Principal component analysis revealed distinct differences in disease characteristics between the keratinized cases and the nonkeratinized control cases, with the keratinized cases exhibiting a significant upregulation of 1272 genes and a significant downregulation of 1846 genes (Fig. 3). On the genes that were significantly upregulated, enrichment analysis was performed using Metascape (Fig. 3), a web-based portal used for cross-sectional analysis of enrichment in each GO term, KEGG (Kyoto Encyclopedia of Genes and Genomes), and canonical pathway classification. The GO term was

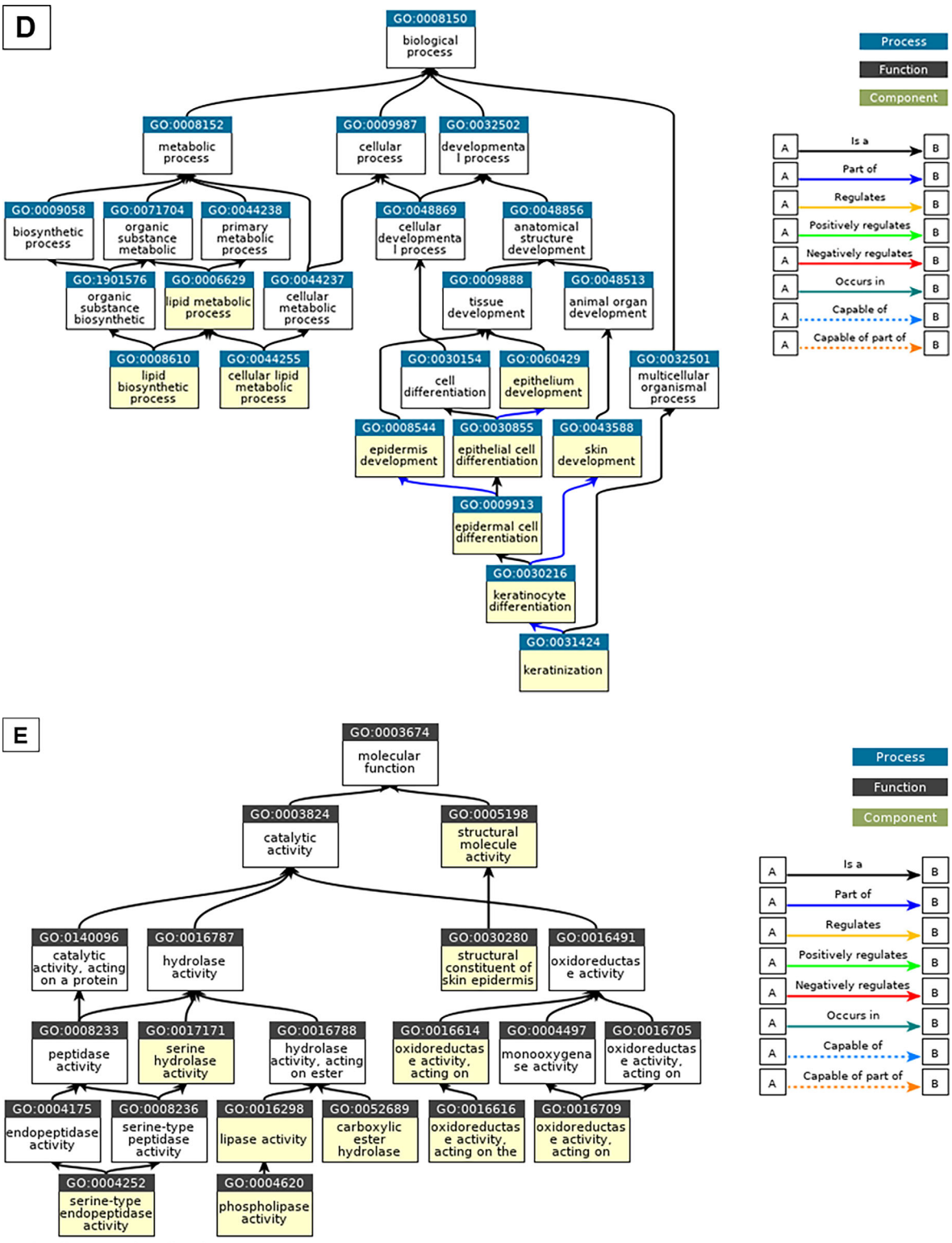

Figure 3. Continued.

assigned to classify genes based on their biological functions and other factors, and the same analysis was performed for genes with significantly decreased expression (Supplementary Fig. S1). In addition, on the genes that were significantly upregulated, GO analysis using DAVID allowed for identification of what kind of biological process or the molecular function of genes whose expression has changed by analyzing how many genes belong to a category with similar function based on the GO term. The 10 GO terms were charted with the lowest *P* values in each category of Biological Process and Molecular Function (Fig. 3). The same analysis was performed for the genes

Table 1A. Transcripts Upregulated in the Keratinized Conjunctival Epithelium

Fold Change	*P* Value	Public Gene IDs	Gene Symbol	Description
9613.76	7.69E-11	NM_001244847	KRTDAP	Keratinocyte differentiation-associated protein
8579.93	5.02E-07	NM_006121	KRT1	Keratin 1, type II
5827.96	3.44E-05	NM_002016	FLG	Filaggrin
5769.91	6.58E-06	NM_001166034	SBSN	Suprabasin
5267.29	0.0005	NM_001014342	FLG2	Filaggrin family member 2
3554.39	5.93E-08	NM_000427	LOR	Loricrin
2019.41	0.0016	NM_002963	S100A7	S100 calcium binding protein A7
1923.08	5.09E-06	NM_019060	CRCT1	Cysteine rich C-terminal 1
1626.71	1.91E-05	NM_012114	CASP14	Caspase 14
1609.66	1.62E-07	NM_006919	SERPINB3	Serpin peptidase inhibitor, clade B (ovalbumin), member 3
1338.83	3.43E-06	NM_174932	BPIFC	BPI fold containing family C
994.74	8.46E-07	NM_001012964; NM_001012965; NM_002774	KLK6	Kallikrein related peptidase 6
991.9	2.04E-06	NM_173483	CYP4F22	Cytochrome P450, family 4, subfamily F, polypeptide 22
941	5.46E-06	NM_002638	PI3	Peptidase inhibitor 3, skin-derived
813.1	1.64E-05	NM_001127698; NM_001127699; NM_006846	SPINK5	Serine peptidase inhibitor, Kazal type 5
803.59	0.0018	NM_016190	CRNN	Cornulin
664.75	4.92E-07	NM_002974; NM_175041	SERPINB4	Serpin peptidase inhibitor, clade B (ovalbumin), member 4
627.28	2.82E-07	NM_018004	TMEM45A	Transmembrane protein 45A
615.49	0.0004	NM_004948; NM_024421	DSC1	Desmocollin 1
602.44	6.76E-06	NM_001258333; NM_001258334; NM_002108	HAL	Histidine ammonia-lyase
596.94	3.22E-08	NM_001307928; NM_080474	SERPINB12	Serpin peptidase inhibitor, clade B (ovalbumin), member 12
441.04	3.14E-06	NM_001011709	PNLIPRP3	Pancreatic lipase-related protein 3
409.7	5.56E-05	NM_016321	RHCG	Rh family, C glycoprotein
406.17	6.79E-06	NM_025261	LY6G6C	Lymphocyte antigen 6 complex, locus G6C
400.81	7.60E-08	NM_032488	CNFN	Cornifelin
385.9	2.00E-07	NM_001077491; NM_001077492; NM_012427	KLK5	Kallikrein related peptidase 5
354.35	9.20E-08	NM_001024209	SPRR2E	Small proline-rich protein 2E
352.9	1.22E-06	NM_000067; NM_001293675	CA2	Carbonic anhydrase II
323.31	5.03E-06	NM_006945	SPRR2D	Small proline-rich protein 2D
316.16	8.30E-06	NM_022726	ELOVL4	ELOVL fatty acid elongase 4
313.73	0.0003	NM_014058	TMPRSS11E	Transmembrane protease, serine 11E
303.19	3.18E-05	NM_001207053; NM_001243126; NM_005046; NM_139277	KLK7	Kallikrein related peptidase 7

The 32 transcripts upregulated more than 300 times and showed significant differences (ANOVA $P < 0.05$) in the keratinized conjunctival epithelium.

in which expression was significantly decreased (Supplementary Fig. S1). Genes involved in keratinization, lipid metabolism, and oxidoreductase were upregulated, while those involved in cellular response, TFs, and the immune system were downregulated (Fig. 3, Supplementary Fig. S1). In addition, 32 transcripts were upregulated more than 300-fold, and 12 transcripts were downregulated less than one-hundredth as genes with particularly large expression changes (Tables 1A and 1B). Among the 32 genes that were most highly upregulated, 21 of the 32 transcripts were genes that are clearly involved in keratinocyte differentiation and cornification. The genes that were highly downregulated included polymeric immunoglobulin receptor (PIGR), clusterin (CLU), and paired box 6 (PAX6).

DNA-Templated Transcription

To clarify the pathogenesis of pathological keratinization, we focused on the trends of TFs that regulate the expression of many genes. We extracted genes related to DNA-templated genes from GO term as TF-related genes, and found 61 genes significantly upregulated and 216 genes significantly downregulated in the microarray. Enrichment analysis was performed on the significantly upregulated and downregulated genes using ChIP-Atlas to identify the upstream TFs. Refining our microarray data with the results of the enrichment analysis identified 4 transcripts for upregulated TFs and 56 transcripts for downregulated TFs. The upregulated TFs in this study included MYB proto-oncogene-like 2 (MYBL2) and forkhead box M1 (FOXM1), which are involved in cell-cycle progression, and sterol regulatory element binding TF 2 (SREBF2), which is considered a master TF for adipocyte differentiation, while E74 like ETS TF 3 (ELF3), which is involved in maintaining normal epidermal cells, was highly downregulated (Tables 2A and 2B).

Vitamin A–Related Transcriptions

We investigated the metabolism and receptors of vitamin A, which is known to suppress cell keratinization. We analyzed the expression of 65 genes in this comprehensive gene expression analysis using the GO term as a reference for

Investigative Ophthalmology & Visual Science

Table 1B. Transcripts Downregulated in the Keratinized Conjunctival Epithelium

Fold Change	*P* Value	Public Gene IDs	Gene Symbol	Description
−975.17	1.83E-05	NM_002644	PIGR	Polymeric immunoglobulin receptor
−797.06	3.11E-06	NM_001177998; NM_001177999; NM_006424	SLC34A2	Solute carrier family 34 (type II sodium/phosphate cotransporter), member 2
−393.2	8.80E-09	NM_000096	CP	Ceruloplasmin (ferroxidase)
−291.15	1.70E-06	NM_001201546; NM_001201547; NM_001201548; NM_001201549; NM_004696	SLC16A4	Solute carrier family 16, member 4
−254.75	1.28E-07	NM_001177355; NM_005823; NM_013404	MSLN	Mesothelin
−254.62	3.00E-06	NM_005727	TSPAN1	Tetraspanin 1
−193.1	3.11E-06	NM_181644	MFSD4	Major facilitator superfamily domain containing 4
−174.79	4.81E-05	NM_001775	CD38	CD38 molecule
−163.27	3.36E-05	NM_001831	CLU; MIR6843	Clusterin; microRNA 6843
−147.98	0.0007	NM_001112706; NM_033128	SCIN	Scinderin
−141.56	0.0043	NM_000280; NM_001127612; NM_001258462; NM_001258463; NM_001258464; NM_001258465; NM_001310158; NM_001310159; NM_001310160; NM_001310161; NM_001604	PAX6	Paired box 6
−104.59	0.0056	NM_006186	NR4A2	Nuclear receptor subfamily 4, group A, member 2

The 12 transcripts downregulated less than 1/100 and showed significant differences (ANOVA $P < 0.05$).

Table 2A. Transcripts Associated with DNA-Binding Transcription Factor Activity, and Representative Transcripts that are Upregulated in Keratinizing Conjunctival Epithelium

Fold Change	*P* Value	Public Gene IDs	Gene Symbol	Description
7	0.0013	NM_001278610; NM_002466	MYBL2	Sterol regulatory element binding transcription factor 2
3.68	0.0008	NM_004599	SREBF2	V-myb avian myeloblastosis viral oncogene homolog-like 2
3.46	0.0054	NM_001243088; NM_001243089; NM_021953; NM_202002; NM_202003	FOXM1	Histone deacetylase 1
2.18	0.0022	NM_004964	HDAC1	Forkhead box M1

DNA-templated genes (GO0006351-5) were extracted from the GO term as those related to transcription factors, and among them, four genes that were significantly upregulated in the microarray and were included in the transcription factors that were speculated to be upregulated were identified by enrichment analysis using ChIP-Atlas from differentially expressed genes in the microarray. ANOVA $P < 0.05$ was considered a significant difference.

genes involved in vitamin A metabolism and receptors. As a result, significant expression changes were observed in 18 genes, of which 12 genes were upregulated and 6 genes were downregulated (Tables 3A and 3B). Binding of vitamin A to nuclear receptors occurs when vitamin A is taken up by epithelial cells as retinol, which is then oxidized to retinal and then retinoic acid (RA), which binds to cellular retinoic acid-binding protein 2 (CRABP2) and acts as a ligand for nuclear receptors. The differentially expressed genes were found to have increased mRNA for enzymes that reduce RA, the active form of vitamin A, and convert it to its inactive forms, retinol and then retinyl esters. On the other hand, the expression of CRABP2, which allows RA to be taken up by nuclear RA receptors (RARs), was significantly upregulated, while the expression of fatty acid binding protein 5, which competes with CRABP2 to bind RA to peroxisome proliferator-activated receptors, was significantly downregulated. Interestingly, the expression of RAR-beta (RARB) was selectively downregulated, while the expression of RAR-alpha (RARA) and RAR-gamma (RARG) was not significantly altered. In addition, when representative genes such as aldo-keto reductase family 1 member (AKR1)-B15 (AKR1B15), AKR1-B10 (AKR1B10), retinol dehydrogenase-12 (RDH12), CRABP2, RAR responder (RARRES) protein 3 (RARRES3), and RARB, whose expression varied more than 10-fold, were examined, there was little difference in expression of the transcripts because of disease (Fig. 4).

QRT-PCR Analysis

For comparison of the upregulated and downregulated transcripts in the epithelium from patients with keratinization and the controls, we performed qRT-PCR on the three keratinization cases and the three nonkeratinization controls in this study to confirm the expression of vitamin A-related transcripts whose expression was significantly changed in the comprehensive gene expression analysis. In this study, qRT-PCR was also performed for AKR1B15, RDH12, AKR1B10, and CRABP2, which are upregulated more than twentyfold among the significantly-upregulated genes and promote binding to RAR, two genes (RARB and RARRES3)

Investigative Ophthalmology & Visual Science

Table 2B. Transcripts Associated with DNA-Binding Transcription Factor Activity, and Representative Transcripts that are Downregulated in Keratinizing Conjunctival Epithelium

Fold Change	*P* Value	Public Gene IDs	Gene Symbol	Description
−52.24	1.54E-05	NM_001114309; NM_004433	ELF3	E74-like factor 3 (ets domain transcription factor, epithelial-specific)
−24.07	4.55E-06	NM_001105539; NM_001277145; NM_023929	ZBTB10	Zinc finger and BTB domain containing 10
−23.05	0.015	NM_001114171; NM_006732	FOSB	FBJ murine osteosarcoma viral oncogene homolog B
−22	0.0042	NM_001030287; NM_001040619; NM_001206484; NM_001206486; NM_001206488; NM_001674	ATF3	Activating transcription factor 3
−15.41	0.0007	NM_001105077; NM_001105078; NM_001163999; NM_001164000; NM_001205194; NM_004991; NM_005241	MECOM	MDS1 and EVI1 complex locus
−15.34	0.0008	NM_004496	FOXA1	Forkhead box A1
−15.01	1.82E-06	NM_001145155; NM_001145156; NM_001145157; NM_021005	NR2F2	Nuclear receptor subfamily 2, group F, member 2
−9.34	4.62E-05	NM_014323; NM_032050; NM_032051; NM_032052	PATZ1	POZ (BTB) and AT hook containing zinc finger 1
−8.13	0.0064	NM_001164342; NM_001164343; NM_001164344; NM_001164345; NM_001164346; NM_001164347; NM_015642	ZBTB20; MIR568	Zinc finger and BTB domain containing 20; microRNA 568
−7.49	7.42E-05	NM_002198	IRF1	Interferon regulatory factor 1
−7.22	0.0004	NM_001206	KLF9	Kruppel-like factor 9
−6.96	0.0081	NM_001964	EGR1	Early growth response 1
−6.57	0.0001	NM_001430	EPAS1	Endothelial PAS domain protein 1
−6.18	3.26E-05	NM_001145102; NM_001145103; NM_001145104; NM_005902	SMAD3	SMAD family member 3
−5.54	4.00E-05	NM_000246; NM_001286402; NM_001286403	CIITA	Class II, major histocompatibility complex, transactivator
−5.26	0.0093	NM_001015051; NM_001024630; NM_001278478	RUNX2	Runt-related transcription factor 2
−4.95	6.41E-05	NM_002199	IRF2	Interferon regulatory factor 2
−4.7	0.0196	NM_032575	GLIS2	GLIS family zinc finger 2
−3.98	0.0009	NM_001204961; NM_001204963; NM_002585	PBX1	Pre-B-cell leukemia homeobox 1
−3.85	0.0046	NM_001453	FOXC1	Forkhead box C1
−3.77	0.0001	NM_007146	VEZF1	Vascular endothelial zinc finger 1
−3.6	0.0118	NM_001079526; NM_016260	IKZF2	IKAROS family zinc finger 2
−3.59	0.001	NM_000449; NM_001025603	RFX5	Regulatory factor X, 5 (influences HLA class II expression)
−3.37	0.0006	NM_001130845; NM_001134738; NM_001706	BCL6	B-cell CLL/lymphoma 6
−3.34	0.0007	NM_005253	FOSL2	FOS-like antigen 2
−3.24	0.0015	NM_003670	BHLHE40	Basic helix-loop-helix family, member e40
−2.96	0.0018	NM_006084	IRF9	Interferon regulatory factor 9
−2.7	0.004	NM_005349; NM_015874; NM_203283; NM_203284OTTHUMT00000215047	RBPJ	Recombination signal binding protein for immunoglobulin kappa J region
−2.67	0.0112	NM_001101802; NM_016621	PHF21A	PHD finger protein 21A
−2.56	0.0055	NM_024671	ZNF768	Zinc finger protein 768
−2.53	0.0052	NM_001166693; NM_005935	AFF1	AF4/FMR2 family, member 1
−2.39	0.0153	NM_001184772; NM_021946	BCORL1	BCL6 corepressor-like 1
−2.34	0.0025	NM_001245002; NM_001245004; NM_001245005; NM_005597; NM_205843	NFIC	Nuclear factor I/C (CCAAT-binding transcription factor)
−2.32	0.0313	NM_002467	MYC	V-myc avian myelocytomatosis viral oncogene homolog
−2.3	0.0099	NM_001206794; NM_016374; NM_031371	ARID4B	AT rich interactive domain 4B (RBP1-like)
−2.25	0.0094	NM_017617	NOTCH1	Notch 1
−2.24	0.0024	NM_002892; NM_023000; NM_023001	ARID4A	AT rich interactive domain 4A (RBP1-like)

Investigative Ophthalmology & Visual Science

Table 2B. Continued

Fold Change	*P* Value	Public Gene IDs	Gene Symbol	Description
−2.22	0.0052	NM_001286818; NM_001730	KLF5	Kruppel-like factor 5 (intestinal)
−2.19	0.0036	NM_001271068; NM_001271069; NM_002382; NM_145112; NM_145113; NM_145114; NM_197957	MAX	MYC associated factor X
−2.18	0.0014	NM_001184896; NM_001184897; NM_001184898; NM_015107	PHF8	PHD finger protein 8
−2.17	0.0402	NM_001039920; NM_001135734; NM_133476	ZNF384	Zinc finger protein 384
−2.15	0.0046	NM_014663	KDM4A	Lysine (K)-specific demethylase 4A
−2.1	0.014	NM_001197104; NM_005933	KMT2A	Lysine (K)-specific methyltransferase 2A
−2.1	0.0177	NM_001987	ETV6	Ets variant 6
−2.07	0.0134	NM_001303425; NM_001303426; NM_016331	ZNF639	Zinc finger protein 639
−2.06	0.0172	NM_001012505; NM_001244808; NM_001244810; NM_001244812; NM_001244813; NM_001244814; NM_001244815; NM_001244816; NM_032682	FOXP1	Forkhead box P1
−2.06	0.0059	NM_001003688; NM_005900	SMAD1	SMAD family member 1
−2.05	0.0069	NM_001267039; NM_015454; NM_016648	LARP7	La ribonucleoprotein domain family, member 7

DNA-templated genes (GO0006351-5) were extracted from the GO term as those related to transcription factors, and among them, 56 genes that were significantly downregulated in the microarray and were included in the transcription factors that were speculated to be downregulated were identified by enrichment analysis using ChIP-Atlas from differentially expressed genes in the microarray. ANOVA $P < 0.05$ was considered a significant difference.

Table 3A. Representative Transcripts Related to Vitamin A and Upregulated in Keratinizing Conjunctival Epithelium

Fold Change	*P*-Value	Public Gene IDs	Gene Symbol	Description
136.09	0.0002	NM_001080538	AKR1B15	Aldo-keto reductase family 1, member B15
102.35	8.82E-07	NM_152443	RDH12	Retinol dehydrogenase 12 (all-trans/9-cis/11-cis)
80.07	0.0001	NM_020299	AKR1B10	Aldo-keto reductase family 1, member B10 (aldose reductase)
24.88	0.0005	NM_001199723; NM_001878	CRABP2	Cellular retinoic acid binding protein 2
8.17	0.0071	NM_001253908; NM_001253909; NM_003739	AKR1C3	Aldo-keto reductase family 1, member C3
7.22	0.0114	NM_001301645; NM_004744	LRAT	Lecithin retinol acyltransferase (phosphatidylcholine–retinol O-acyltransferase)
7.03	0.0182	NM_001135241; NM_001354; NM_205845	AKR1C2	Aldo-keto reductase family 1, member C2
6.02	0.0132	NM_001243325; NM_001243327; NM_001243328; NM_139165	RAET1E	Retinoic acid early transcript 1E
4.42	0.0053	NM_130900	RAET1L	Retinoic acid early transcript 1L
3.88	0.0002	NM_052960	RBP7	Retinol binding protein 7, cellular
3.01	0.0031	NM_001252650; NM_016026	RDH11	Retinol dehydrogenase 11 (all-trans/9-cis/11-cis)
2.06	0.0321	NM_001818	AKR1C4	Aldo-keto reductase family 1, member C4

We analyzed the expression of 65 genes in this comprehensive gene expression analysis, using the GO term as a reference for genes involved in vitamin A metabolism and receptors. Twelve genes that were significantly upregulated and showed significantly differences (ANOVA $P < 0.05$).

whose expression were downregulated less than 1/50, and RARA and RARG, which are other RAR types. The results of the qRT-PCR were similar to the results of the comprehensive gene expression analysis.

Similar to the results of the comprehensive gene expression analysis, AKR1B15, RDH12, AKR1B10, and CRABP2 were significantly upregulated in the keratinized cases. On the other hand, RARB and RARRES3 mRNAs were significantly downregulated, while RARA and RARG mRNAs showed no significant changes in expression (Fig. 5).

Discussion

To the best of our knowledge, this is the first study to clarify the relationship between pathological keratinization. The expression of 3118 genes in keratinized epithelial cells was significantly upregulated compared to controls. The

Investigative Ophthalmology & Visual Science

Table 3B. Representative Transcripts Related to Vitamin A and Downregulated in Keratinizing Conjunctival Epithelium

Fold Change	*P*-Value	Public Gene IDs	Gene Symbol	Description
−59.12	1.41E-07	NM_000965; NM_001290216; NM_001290217; NM_001290266; NM_001290276; NM_001290277; NM_001290300; NM_016152	RARB	Retinoic acid receptor, beta
−54.18	1.55E-08	NM_004585	RARRES3	Retinoic acid receptor responder (tazarotene induced) 3
−5.1	0.0158	NM_001145520; NM_001145521; NM_001145522; NM_001145523; NM_001145525; NM_015577	RAI14	Retinoic acid induced 14
−4.11	0.009	NM_000689	ALDH1A1	Aldehyde dehydrogenase 1 family, member A1
−2.9	0.0002	NM_001202413; NM_001202414; NM_006066; NM_153326	AKR1A1	Aldo-keto reductase family 1, member A1 (aldehyde reductase)
−2.29	0.0099	NM_030665	RAI1	Retinoic acid induced 1

We analyzed the expression of 65 genes in this comprehensive gene expression analysis, using the GO term as a reference for genes involved in vitamin A metabolism and receptors. Six genes that were significantly downregulated and showed significantly differences (ANOVA $P < 0.05$).

upregulated transcripts were enriched with genes involving keratinization and lipid metabolism, while the downregulated transcripts were enriched with genes involving immune response and TFs. The most predominantly differentially expressed genes were associated with keratinization. PAX6 and CLU, which are known to be downregulated in OSDs, were also significantly downregulated. Interestingly, the expression of genes related to vitamin A metabolism and signaling pathways were also significantly differentiated.[13] This may play an important role in the cause of cases of OS pathological keratinization.

RA is produced from vitamin A through two sequential oxidation steps,[14] and vitamin A is an essential nutrient required for embryogenesis, determining cell lineage, and fate commitment.[15–17] RA is a ligand transduced by two types of nuclear receptors, RAR and RXR (retinoid X receptor), both of which composed of three isotypes, alpha, beta, and gamma,[16] and it is attributed to the trans-repression of keratinization by RAR stimulation in OS cells.[18] In this study, the expression of RARB was significantly decreased, yet there was no significant change in the expression of RARA and RARG, the receptors for vitamin A. The uptake of RA into the nuclear receptors of RARs was likely enhanced by the increase in CRABP2 and the decrease in FABP5.[19,20] However, RA seemed to be decreased because the expression of enzymes that convert RA, an active vitamin A, to inactive forms, such as retinal, retinol, and retinyl esters, was increased, and decreased expression of transcripts was induced by RA such as RARB, RARRES, and PAX6.[19,21–24] In addition, the expression of genes related to vitamin A was significantly different, and although the number of cases was limited, there were few differences in the expression of transcripts because of disease (i.e., OCP, SJS, anterior staphyloma).

RARB is reportedly upregulated by RA, and plays a very important role in ocular development.[15–17] Although the role of RARB on the OS after development has yet to be fully elucidated in detail, its expression is decreased in some malignant tumors. It has been reported that decreased RARB expression correlates with keratinization in premalignant oral lesions and squamous cell carcinoma of the head and neck, and that the expression of RARB or stimulation with pharmacological doses of vitamin A converts the keratinized cell phenotype into nonkeratinized cells.[25–27] In this study, we found that significantly lower RARB expression correlated with keratinization in pathological keratinized compared to nonkeratinized conjunctival epithelium.

It is known that vitamin A inhibits squamous metaplasia of corneal limbal stem cells in late cultures in vitro.[18,28] The efficacy of topically administered vitamin A as a therapeutic agent to reduce OS keratinization has previously been reported, and there have been attempts to use it as a novel therapeutic agent in SJS cases. However, even with topical treatment, side effects such as meibomian gland inflammation and keratitis have been reported, and it has not yet reached any practical use in the clinical setting.[29–31] Recently, a report regarding the safety and efficacy of retinol palmitate ophthalmic solution for SJS with OS keratinization is of great interest.[29] We consider it necessary to use more specific ligands such as RARB as therapeutic agents and to find new therapeutic targets by clarifying the causes of decreased expression of only RARB.

The TF differentially expressed genes in this study may reflect the pathogenesis of pathological keratinization. SREBF2, whose expression was upregulated, is a TF related to cholesterol synthesis that is known to contribute to cornification in the epidermis.[32,33] In pathological keratinization, the OS is significantly keratinized, which may reflect the formation of cornified layer. Furthermore, it is involved in keratinocyte differentiation through lipid synthesis, and its expression is suppressed with RA inhibition of keratinization.[34] It is known that MYBL2, a member of the MYN TF family, is overexpressed in malignant tumors, and its expression is involved in cell proliferation and cell-cycle progression.[35] FOXM1 is a TF known to regulate mainly the G2/M phase. In ophthalmology, it reportedly plays an important role in the pathogenesis of pterygium, and it has functions such as cell proliferation and maintenance of stemness.[36,37] The histone deacetylase HDAC1 is considered a fibrogenesis acceleration and a proinflammatory molecule on the OS. Therefore it is considered as a therapeutic target for the prevention of symblepharon.[38] These TFs may be highly relevant to the regulation of OS cell turnover in pathological keratinization.

Investigative Ophthalmology & Visual Science

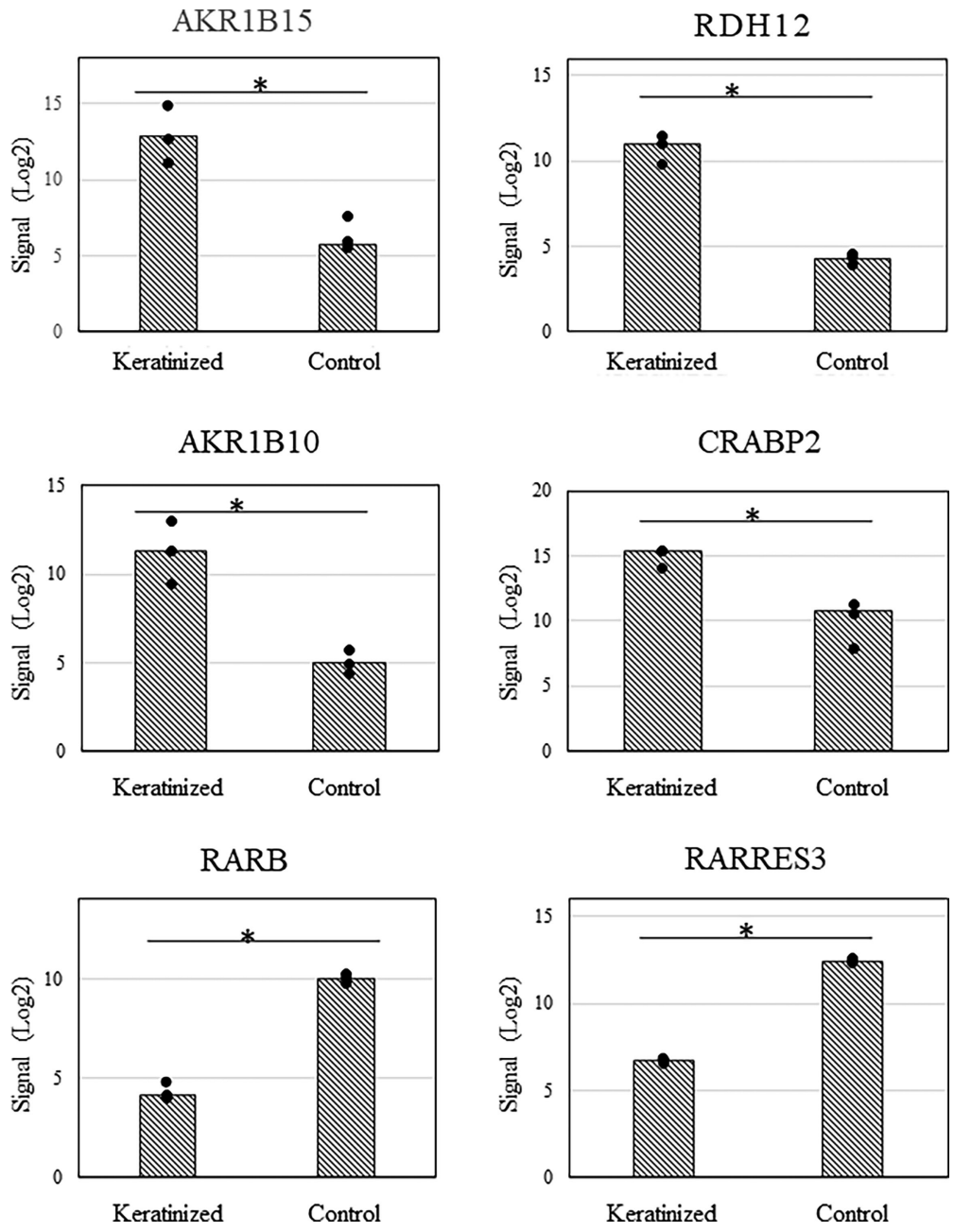

Figure 4. Graphs showing the results of the representative transcripts of significantly differentially expressed genes related to vitamin A metabolism in microarrays. Representative genes AKR1B15, RDH12, AKR1B10, CRABP2, RARRES3, and RARB up- or downregulated more than tenfold in normalized signal among 65 genes related to vitamin A metabolism and receptors based on GO term. Little difference was found in these transcripts for each disease.

ELF3 is one of the epithelium-specific ETS TFs defined by their highly conserved ETS DNA binding domain and predominant epithelial-specific expression profile.[39,40] On the OS, ELF3 is reportedly expressed in the corneal epithelium and goblet cells. FOSB (FBJ murine osteosarcoma viral, oncogene homolog B), ATF3 (activating transcription factor 3), and EGR1 (early growth response protein 1), which are reportedly downregulated in pterygium, were also downregulated in this analysis.[41] These may be involved in normal tissue homeostasis. To the best of our knowledge, there are no previous reports of these upregulated TFs being involved in disease. Thus these TFs may provide novel targets for understanding the pathogenesis and treatment of keratinization.

We previously reported that CLU and PAX6 are downregulated in pathological keratinization and that the expression of genes related to epidermis development is upregulated and PIGR expression is downregulated in SJS.[13,42] Reportedly, the expression of aldehyde dehydrogenase 1 family member 1 (ALDH1) is elevated in OCP cases and is associated with fibrosis.[43] In this study, ALDH1 upregulation was common in OCP, and these findings are consistent with the results of the present comprehensive gene expression analysis.

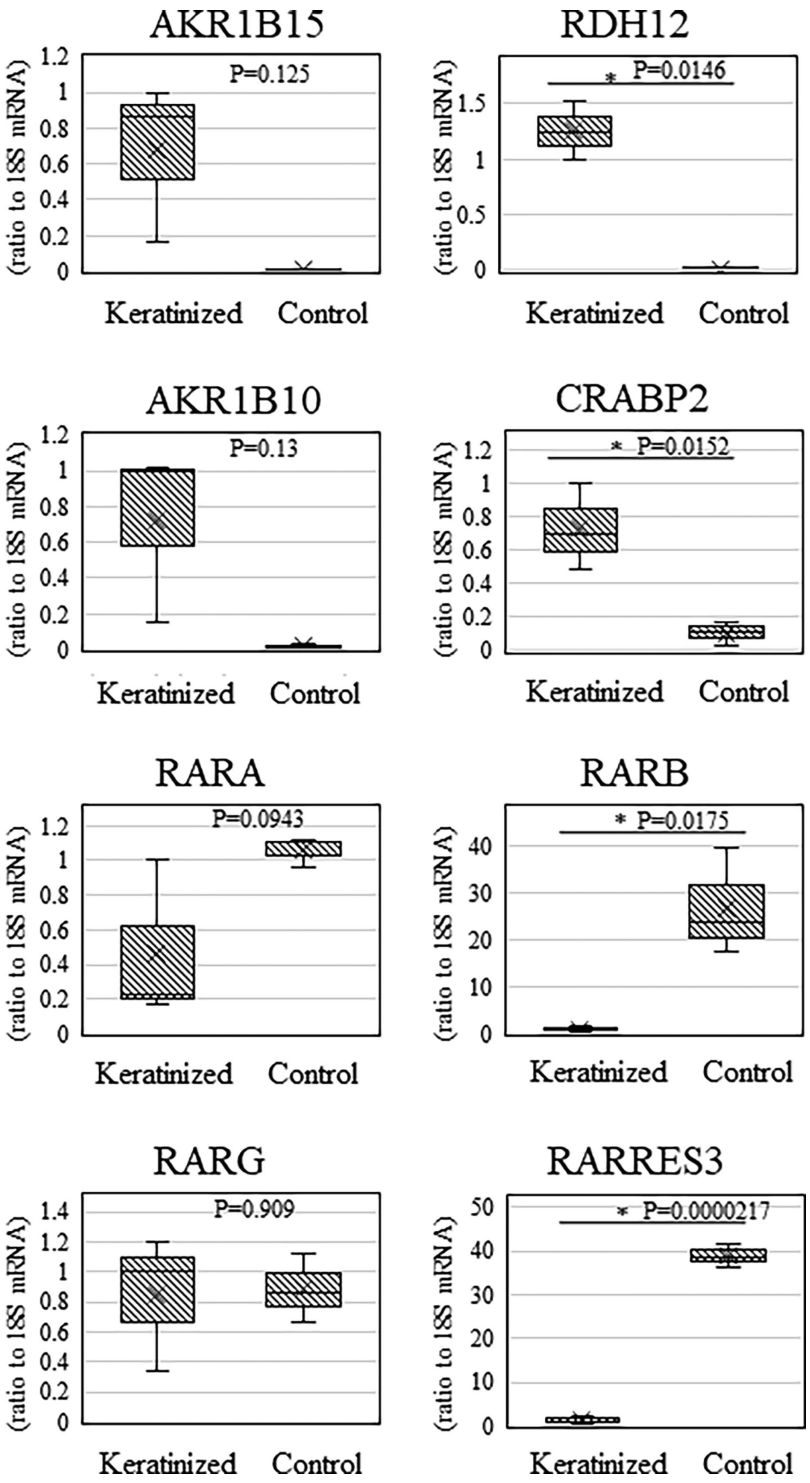

Figure 5. Graphs showing the representative transcripts of genes related to vitamin A metabolism in qRT-PCR. QRT-PCR was also performed for the genes AKR1B15, RDH12, AKR1B10, and CRABP2, which are upregulated more than twentyfold among the significantly upregulated genes and promote binding to RAR, two genes (RARB and RARRES3) whose expression was downregulated more than 1/50, and RARA and RARG, which are other types of RAR. By normalizing the expression of the gene of interest to the expression of 18S rRNA, we were able to obtain a relative measure of the expression level of each gene (*$P < 0.05$, **$P < 0.005$, ***$P < 0.0005$). Similar to the microarray results, RARB, CRABP2, and RARRES3 showed significant differences, whereas RARA and RARG showed no significant differences.

We found that genes involved in keratinization were significantly upregulated in conjunctival epithelium, while expression of genes involved in OS immune system, including PIGR, was significantly downregulated.[42] In addition, we found that TFs thought to be involved in differentially expressed genes were downregulated.

Limitations of the present study were the low number of cases analyzed and the significant difference in the age of

Investigative Ophthalmology & Visual Science

keratinized cases due to the age at onset of disease characteristics. The diseases recruited for this study are rare, and it is difficult to perform OS reconstruction surgery for an OSD with pathological keratinization. However, we were fortunately able to apply cultivated oral mucosal epithelial transplantation in challenging cases. In addition, the samples in this study were of different diseases and different patient ages and it can be assumed that the pathophysiology leading to keratinization is also different from the pattern of gene expression, but they have a common pathology of keratinization. In the future, further investigation involving a larger number of cases is needed for a broader clarification of the pathogenesis of the keratinization. In conclusion, the findings in this study suggest that the pathological keratinization of the OS involves cell proliferation, keratinization, and increased lipid synthesis and that decreased expression of RARB may be involved in this pathology.

Acknowledgments

The authors thank John Bush for the critical reading of this manuscript, and Hiromi Nishigaki for technical assistance with the experiments.

Supported by grants from the Japan Agency for Medical Research and Development (AMED) (Grant No. JP23ek0109572h0003) and grants from the Japanese Ministry of Education, Culture, Sports, Science and Technology Scientific Research (B) (Grant No. JP22h03244).

Disclosure: **H. Yoshioka**, None; **M. Ueta**, None; **H. Fukuoka**, None; **N. Yokoi**, None; **K. Mizushima**, None; **Y. Naito**, None; **S. Kinoshita**, None; **C. Sotozono**, None

References

1. Deng SX, Borderie V, Chan CC, et al. Global consensus on definition, classification, diagnosis, and staging of limbal stem cell deficiency. *Cornea.* 2019;38:364–375.
2. Kohanim S, Palioura S, Saeed HN, et al. Acute and chronic ophthalmic involvement in Stevens-Johnson syndrome/toxic epidermal necrolysis—a comprehensive review and guide to therapy. II. Ophthalmic disease. *Ocul Surf.* 2016;14:168–188.
3. Dart JK. The 2016 Bowman Lecture Conjunctival curses: scarring conjunctivitis 30 years on. *Eye (Lond).* 2017;31:301–332.
4. Yoshikawa Y, Ueta M, Fukuoka H, et al. Long-term progression of ocular surface disease in Stevens-Johnson syndrome and toxic epidermal necrolysis. *Cornea.* 2020;39:745–753.
5. Jain R, Sharma N, Basu S, et al. Stevens-Johnson syndrome: the role of an ophthalmologist. *Surv Ophthalmol.* 2016;61:369–399.
6. Elder MJ, Bernauer W, Leonard J, Dart JK. Progression of disease in ocular cicatricial pemphigoid. *Br J Ophthalmol.* 1996;80:292–296.
7. Santos MS, Gomes JA, Hofling-Lima AL, Rizzo LV, Romano AC, Belfort R, Jr. Survival analysis of conjunctival limbal grafts and amniotic membrane transplantation in eyes with total limbal stem cell deficiency. *Am J Ophthalmol.* 2005;140:223–230.
8. Di Girolamo N, Park M. Cell identity changes in ocular surface Epithelia. *Prog Retin Eye Res.* 2022;95:101148.
9. Fogagnolo P, De Cilla S, Alkabes M, Sabella P, Rossetti L. A review of topical and systemic vitamin supplementation in ocular surface diseases. *Nutrients.* 2021;13:1998.
10. Komai S, Inatomi T, Nakamura T, et al. Long-term outcome of cultivated oral mucosal epithelial transplantation for fornix reconstruction in chronic cicatrising diseases. *Br J Ophthalmol.* 2021;106:1355–1362.
11. Wan Y, Xiao G, Yu T, Zhang P, Hong J. Histopathological examination of congenital corneal staphyloma and prognosis after penetrating keratoplasty. *Medicine (Baltimore).* 2020;99:e21892.
12. Kanda Y. Investigation of the freely available easy-to-use software 'EZR' for medical statistics. *Bone Marrow Transplant.* 2013;48:452–458.
13. Nakamura T, Nishida K, Dota A, Kinoshita S. Changes in conjunctival clusterin expression in severe ocular surface disease. *Invest Ophthalmol Vis Sci.* 2002;43:1702–1707.
14. Carazo A, Macakova K, Matousova K, Krcmova LK, Protti M, Mladenka P. Vitamin A update: forms, sources, kinetics, detection, function, deficiency, therapeutic use and toxicity. *Nutrients.* 2021;13:1703.
15. Clagett-Dame M, Knutson D. Vitamin A in reproduction and development. *Nutrients.* 2011;3:385–428.
16. Lohnes D, Mark M, Mendelsohn C, et al. Function of the retinoic acid receptors (RARs) during development (I). Craniofacial and skeletal abnormalities in RAR double mutants. *Development.* 1994;120:2723–2748.
17. Matt N, Ghyselinck NB, Pellerin I, Dupe V. Impairing retinoic acid signalling in the neural crest cells is sufficient to alter entire eye morphogenesis. *Dev Biol.* 2008;320:140–148.
18. Samarawickrama C, Chew S, Watson S. Retinoic acid and the ocular surface. *Surv Ophthalmol.* 2015;60:183–195.
19. Napoli JL. Cellular retinoid binding-proteins, CRBP, CRABP, FABP5: effects on retinoid metabolism, function and related diseases. *Pharmacol Ther.* 2017;173:19–33.
20. Celik SD, Ates O. Analysis of CRABP2 and FABP5 genes in primary and recurrent pterygium tissues. *Mol Biol Rep.* 2020;47:6105–6110.
21. Lee SA, Belyaeva OV, Popov IK, Kedishvili NY. Overproduction of bioactive retinoic acid in cells expressing disease-associated mutants of retinol dehydrogenase 12. *J Biol Chem.* 2007;282:35621–35628.
22. Chung YT, Matkowskyj KA, Li H, et al. Overexpression and oncogenic function of aldo-keto reductase family 1B10 (AKR1B10) in pancreatic carcinoma. *Mod Pathol.* 2012;25:758–766.
23. Endo S, Morikawa Y, Matsunaga T, Hara A, Nishinaka T. Porcine aldo-keto reductase 1C subfamily members AKR1C1 and AKR1C4: substrate specificity, inhibitor sensitivity and activators. *J Steroid Biochem Mol Biol.* 2022;221:106113.
24. Berenguer M, Meyer KF, Yin J, Duester G. Discovery of genes required for body axis and limb formation by global identification of retinoic acid-regulated epigenetic marks. *PLoS Biol.* 2020;18:e3000719.
25. Rotondo JC, Borghi A, Selvatici R, et al. Association of retinoic acid receptor beta gene with onset and progression of lichen sclerosus-associated vulvar squamous cell carcinoma. *JAMA Dermatol.* 2018;154:819–823.
26. Youssef EM, Chen XQ, Higuchi E, et al. Hypermethylation and silencing of the putative tumor suppressor Tazarotene-induced gene 1 in human cancers. *Cancer Res.* 2004;64:2411–2417.
27. Wan H, Oridate N, Lotan D, Hong WK, Lotan R. Overexpression of retinoic acid receptor beta in head and neck squamous cell carcinoma cells increases their sensitivity to retinoid-induced suppression of squamous differentiation by retinoids. *Cancer Res.* 1999;59:3518–3526.
28. Hori Y, Spurr-Michaud SJ, Russo CL, Argueso P, Gipson IK. Effect of retinoic acid on gene expression in human conjunctival epithelium: secretory phospholipase A2 medi-

ates retinoic acid induction of MUC16. *Invest Ophthalmol Vis Sci.* 2005;46:4050–4061.

29. Ravindra AP, Sinha R, Bari A, et al. Retinol palmitate in management of chronic Steven-Johnson Syndrome with ocular surface keratinization. *Ocul Surf.* 2023;30:160–167.
30. Srividya G, Angayarkanni N, Iyer G, Srinivasan B, Agarwal S. Altered retinoid metabolism gene expression in chronic Stevens-Johnson syndrome. *Br J Ophthalmol.* 2019;103:1015–1023.
31. Ubels JL. A retrospective on topical retinoids occasioned by observation of unexpected interactions of retinoic acid with androgens and glucocorticoids in immortalized lacrimal acinar cells. *Exp Eye Res.* 2005;80:281–284.
32. Elias PM. Stratum corneum defensive functions: an integrated view. *J Invest Dermatol.* 2005;125:183–200.
33. Harris IR, Farrell AM, Holleran WM, et al. Parallel regulation of sterol regulatory element binding protein-2 and the enzymes of cholesterol and fatty acid synthesis but not ceramide synthesis in cultured human keratinocytes and murine epidermis. *J Lipid Res.* 1998;39:412–422.
34. Lee DD, Stojadinovic O, Krzyzanowska A, Vouthounis C, Blumenberg M, Tomic-Canic M. Retinoid-responsive transcriptional changes in epidermal keratinocytes. *J Cell Physiol.* 2009;220:427–439.
35. Musa J, Aynaud MM, Mirabeau O, Delattre O, Grunewald TG. MYBL2 (B-Myb): a central regulator of cell proliferation, cell survival and differentiation involved in tumorigenesis. *Cell Death Dis.* 2017;8:e2895.
36. Xu Y, Qiao C, He S, et al. Identification of functional genes in pterygium based on bioinformatics analysis. *Biomed Res Int.* 2020;2020:2383516.
37. Enzo E, Secone Seconetti A, Forcato M, et al. Single-keratinocyte transcriptomic analyses identify different clonal types and proliferative potential mediated by FOXM1 in human epidermal stem cells. *Nat Commun.* 2021;12:2505.
38. Swarup A, Ta CN, Wu AY. Molecular mechanisms and treatments for ocular symblephara. *Surv Ophthalmol.* 2022;67:19–30.
39. Luk IY, Reehorst CM, Mariadason JM. ELF3, ELF5, EHF and SPDEF transcription factors in tissue homeostasis and cancer. *Molecules.* 2018;23:2191.
40. Swamynathan SK, Swamynathan S. Corneal epithelial development and homeostasis. *Differentiation.* 2023;132:4–14.
41. Li J, Tao T, Yu Y, et al. Expression profiling suggests the involvement of hormone-related, metabolic, and Wnt signaling pathways in pterygium progression. *Front Endocrinol (Lausanne).* 2022;13:943275.
42. Ueta M, Sotozono C, Nishigaki H, et al. Gene expression analysis of conjunctival epithelium of patients with Stevens-Johnson syndrome in the chronic stage. *BMJ Open Ophthalmol.* 2019;4:e000254.
43. Ahadome SD, Abraham DJ, Rayapureddi S, et al. Aldehyde dehydrogenase inhibition blocks mucosal fibrosis in human and mouse ocular scarring. *JCI Insight.* 2016;1:e87001.

Investigative Ophthalmology & Visual Science